Materials and Structures/Matériaux et Constructions, Vol. 34, November 2001, pp 557-565

Drying/hydration in cement pastes during curing

D. P. Bentz[1], K. K. Hansen[2], H. D. Madsen[2], F. Vallée[3] and E. J. Griesel[4]

(1) Building and Fire Research Laboratory, 100 Bureau Drive Stop 8621, National Institute of Standards and Technology, Gaithersburg, MD 20899-8621 USA

(2) Technical University of Denmark, Lyngby, Denmark

(3) Centre Scientifique et Technique du Bâtiment, Marne-la-Vallée, France

(4) University of Cape Town, South Africa

Paper received: August 21, 2000; Paper accepted: March 23, 2001

ABSTRACT

As concrete cures in the field, there is a constant competition for the mixing water between evaporation and hydration processes. Understanding the mechanisms of water movement in the drying/hydrating cement paste is critical for designing curing systems and specialized rendering materials, as well as for selecting repair materials and methodologies. In this work, X-ray absorption measurements indicate that fresh cement paste dries uniformly throughout its thickness, as opposed to exhibiting the sharp drying front observed for most porous materials. Furthermore, in layered composite cement paste specimens, water always flows from the coarser-pore layer to the finer one, both when coarser pores are produced by using an increased water-to-cement ratio (w/c) and when they are present due to using a cement with a coarser particle size distribution at a constant w/c. Conversely, no clear differential water movement is observed between layers of cement paste and mortar of the same nominal w/c. Based on the results of these experiments, drying has been introduced into the NIST CEMHYD3D cement hydration and microstructure development model, by emptying the largest water-filled pores present at any depth in the model specimen at a user-specified (drying) rate. With this addition, the CEMHYD3D model produces results in good agreement with experimental observations of both the drying profiles and the hydration kinetics of thin cement paste specimens.

RÉSUMÉ

Lors de la cure du ciment sur chantier, la réaction d'hydratation est en constante compétition avec l'évaporation. La compréhension des mécanismes de mouvements d'eau au sein de la pâte en cours de séchage/hydratation est essentielle non seulement en vue de déterminer des méthodes de cure adaptées et de développer des mortiers spéciaux, mais également en vue de sélectionner les bons produits et les bonnes méthodologies de réparation. Dans ce travail, les mesures d'absorption des rayons X mettent en évidence que la pâte de ciment sèche de façon uniforme sur toute son épaisseur, et non selon un front marqué comme on peut couramment l'observer dans les matériaux poreux. De plus, dans le cas de pâte de ciment bi-couche, les mouvements d'eau se font toujours de la couche contenant les pores de taille la plus importante vers celle contenant les pores les plus fins, que les pores grossiers soient dus à un rapport e/c élevé ou à une granulométrie grossière des particules de ciment. A l'inverse, aucun mouvement d'eau n'est observé entre couches de pâte de ciment et de mortier à rapport e/c constant. Sur la base de ces résultats, le séchage a été introduit dans le modèle d'hydratation et de développement de la microstructure du ciment CEMHYD3D développé par le NIST. Les pores saturés d'eau de tailles les plus importantes sont ainsi vidés selon une cinétique fixée par l'opérateur, ceci quelle que soit leur position dans l'épaisseur de l'échantillon. CEMHYD3D génère ainsi des résultats présentant une bonne corrélation avec les observations expérimentales, en terme de profils de séchage et de cinétiques d'hydratation, réalisées sur des pâtes de ciment de faible épaisseur.

1. INTRODUCTION

To achieve optimal performance from cement-based materials in the field, proper curing conditions must be maintained throughout the first few weeks of their life [1, 2]. Unfortunately, due to a lack of quality control in the field, concretes and mortars often experience considerable drying before the cement paste matrix has undergone "complete" hydration. For some materials, such as the thin cement/polymer composite mortars used as rendering materials, later addition of liquid water to the dried composite is not able to "reinitiate" the cement hydration process [3]. For others, this re-initiation of hydration causes significant internal damage to

Editorial Note

Mr. Dale P. Bentz is a RILEM Senior Member. He works at the NIST (USA), a Titular Member. He is also a Member of RILEM Coordinating Committee and was awarded the Robert L'Hermite medal in 1998. CSTB (France) is a RILEM Titular Member.

1359-5997/01

the microstructure and a loss of mechanical properties [4]. Basic understandings of water movement and the kinetics of both hydration and drying in cement-based materials are thus needed to produce systems with adequate performance. This applies to freshly cast cementitious systems, curing compounds, and repair materials. In this paper, experimental and computer modeling studies are applied to elucidating an understanding of the basic mechanisms of water movement in fresh cement pastes and mortars.

For the experimental studies, use was made of an X-ray environmental chamber that has recently been constructed at the Technical University of Denmark to examine building materials exposed to various drying environments [5]. Both relative humidity and air temperature can be controlled within the chamber, which also serves as a shield from the X-ray source. In this study, the X-ray environmental chamber was used to monitor water movement during the drying of small cement paste and mortar specimens. Because the X-ray absorption is proportional to the density of the materials through which the X-rays are passing, a high water-to-cement ratio (w/c) less dense paste will absorb less X-rays than a lower w/c paste. Similarly, a paste that has dried out will absorb less X-rays than the same paste under its initial saturated conditions, allowing a rapid non-destructive quantification of the moisture distribution within the drying/hydrating sample.

In addition to the experimental studies, the NIST three-dimensional cement hydration and microstructure development computer model [6, 7], CEMHYD3D, has been extended to directly consider drying and the consequences of empty (as opposed to water-filled) porosity on microstructure development and hydration kinetics. Based on the experimental observations, appropriate algorithms were developed for simulating the drying of fresh cement paste and the extended code was applied to simulating several of the systems on which experimental measurements were made [8, 9].

2. EXPERIMENTAL PROCEDURE

Details of the X-ray environmental chamber are provided in Refs. [5] and [8]. The X-ray system consists of an X-ray source, a detector, and a positioning table to move the source and detector relative to the specimen being evaluated. The detector uses an NaI crystal and measures the photon count for each of 256 discrete energy channels. The entire system is computer controlled, so that the user may set up a grid of specimen points to be evaluated at periodic intervals.

For this study, three different cements were used: 1) an ASTM Type I/II ordinary portland cement, issued as Cement 133 in June 1999 by the Cement and Concrete Reference Laboratory at NIST [10], 2) a coarse low C_3A content cement ground to a fineness of 254 m^2/kg (median particle diameter of about 25 μm) [11], and 3) an ultra-fine cement ground to a fineness of 654 m^2/kg (median particle diameter of 5 μm). Cement 133 has a potential Bogue composition of 58.6% C_3S, 14.8% C_2S, 10.6% C_3A, and 7.5% C_4AF based on oxide analysis, with a Blaine fineness of about 350 m^2/kg [10]. The low C_3A cement has a Bogue composition of 59.0% C_3S, 25.9% C_2S, 0.6% C_3A, and 14.2% C_4AF, as determined by quantitative microscopy, with hemihydrate added at a mass fraction of 0.05. For the ultra-fine cement, the Bogue composition (via quantitative microscopy) is 73.5% C_3S, 16.5% C_2S, 7.1% C_3A, and 2.5% C_4AF, once again with a 5.0% by mass hemihydrate addition. Small (50 g to 100 g) samples of cement pastes and mortars were prepared in glass beakers and mixed by hand using a spatula for two to three minutes. In general, cement pastes and mortars of w/c = 0.3 and 0.45 were prepared.

The fresh cement pastes were placed in either small inverted Lego[1] blocks (a common children's toy building block) or larger parallelepiped cuvettes, which were either left open or sealed with a cap. The Lego blocks and plexiglass cuvettes were chosen as sample holders due to: 1) their low absorption of X-rays [9], 2) their inherent stackability (allows repeatable placement of the block within the X-ray chamber), 3) the ease with which they can be sealed by adding a cap, and 4) the ease with which they can be filled with a level volume of the viscous cement paste. The cuvettes have the additional advantage of being transparent, so that the drying behavior may be directly inferred from changes in the "brightness" of the sample. The basic experimental setup, illustrated for the composite (layered) cement paste specimens to be described below in the Results and Discussion section, is shown in Fig. 1.

Each block was labeled and weighed (to ± 0.01 g) before the cement paste was added. The masses of the cement paste-filled blocks were determined initially and periodically throughout the exposure period. The blocks were located sequentially on a holder (an inverted

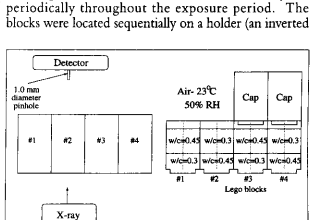

Fig. 1 – Experimental setup for the first layered cement pastes experiment. Image on the left shows a horizontal view of the setup with samples numbered from 1 to 4 and image on the right is a vertical view [8].

(1) Certain commercial equipment is identified in this paper to specify the experimental procedure. In no case does such identification imply endorsement by the National Institute of Standards and Technology, nor does it indicate that the products are necessarily the best available for the purpose.

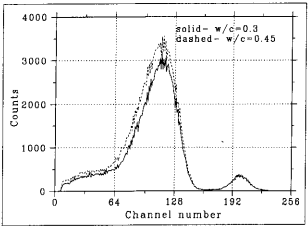

Fig. 2 - Measured spectra for fresh cement pastes [8]. Each channel number corresponds to a discrete energy level.

Lego base element) placed at a fixed location within the X-ray chamber. After specific periods of exposure, the X-ray system was used to scan vertically (in 0.2 mm increments) a distance of either 8 mm (Legos) or 20 mm (cuvettes) along the central y-axis of each block. A five second count time was used at each location to improve the signal to noise ratio. Assuming a Poisson process, the relative standard uncertainty in the sum of the counts obtained for channels 50 to 150 should be on the order of 300 counts or 0.4% (for a sum of 70,000 counts, a typical value for the cement paste specimens).

Examples of spectra measured for two of the fresh cement pastes are provided in Fig. 2. The small peak at channel 200 is from an internal Cobalt source used for system calibration. The denser w/c = 0.3 cement paste is seen to absorb more of the X-rays as indicated by its lower count values at all channels up to 150. Based on the pattern observed in Fig. 2, the sum of counts between channels 50 and 150 was selected as the dependent variable to be analyzed as being representative of the density (and water content) of the cement paste. This value was normalized by dividing it by the ratio of the counts achieved in free air at each measuring time to the counts achieved in free air for the first measuring time (to account for inherent variability in the X-ray source). In the graphs that follow, these normalized counts have been divided by one thousand producing values generally between 70 and 140. In some cases, differential density (counts) profiles have been produced by subtracting the 3 h absorption values at each spatial location from all subsequent readings at the same location, to highlight the changes occurring after the initial setting/settling of the cement paste is complete.

3. COMPUTER MODELING - CEMHYD3D

To adapt the NIST CEMHYD3D cement hydration and microstructure development computer model to examining drying/hydration in fresh cement pastes, several enhancements to the most recent documented version of the code [7] were required. These included a modification of the model boundary conditions, an extension of the model physical dimensions, and the addition of subroutines to implement the actual creation of empty porosity due to the drying.

The previous versions of CEMHYD3D typically simulate the hydration of a 100 pixel x 100 pixel x 100 pixel cubic volume with periodic boundaries along all faces of the volume [7]. To examine drying in thin cement pastes, the periodic boundary conditions at the top and bottom surfaces are removed and movement of model diffusing species across these faces is prohibited. Furthermore, when generating the starting 3-D microstructure, during particle placement, no particles are allowed to protrude across the top and bottom hydration volume surfaces. To simulate approximately the complete thickness of the specimens studied experimentally, the model dimensions are extended to study microstructures either 1000 pixels or 4000 pixels thick. With each pixel 1 μm in dimension, these models systems are thus either 1 mm or 4 mm thick.

Originally, it had been planned to simulate the drying process of a hydrating cement paste by 'intruding' a drying front from the top exposed surface at a user-specified rate. However, the initial X-ray absorption results (to be presented below) indicated that, instead of proceeding as a sharp intruding front, the drying actually occurs relatively uniformly throughout the specimen thickness. It appears that the largest pores everywhere empty first, followed by the next largest, etc. This behavior can be conveniently modeled in the same way that self-desiccation due to chemical shrinkage had previously been implemented in the CEMHYD3D model [6, 12, 13]. To assess the size of the "pores" in the 3-D microstructure, a digitized spherical template (diameter = 13 pixels) is centered at each pixel, and the number of underlying pixels assigned to be water-filled porosity or previously emptied porosity is determined. These values are then sorted from largest to smallest and the largest pores emptied first at a rate determined by a user-supplied drying (rate) datafile. While this algorithm is relatively slow in implementation for a 100 x 100 x 4000 microstructure, it could easily be parallelized to obtain a faster turnaround time on a multi-processor computer.

4. RESULTS AND DISCUSSION

In the first experiment, cement pastes of w/c = 0.3 and 0.45 were prepared and immediately placed in their block molds. While these blocks were exposed to a variety of drying conditions [8], here we shall focus on the set of blocks that was immediately exposed to the chamber environment of 50% RH and 23°C. For these specimens, X-ray measurements were performed over a period of 7 d.

After the initial settling (setting) of the cement paste, surprisingly, the drying profiles are observed to change in a relatively uniform manner throughout the thickness (depth) of the specimen, as shown in Fig. 3. This is in

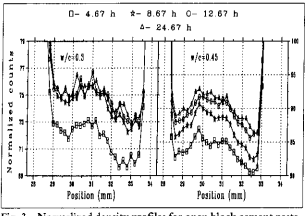

Fig. 3 – Normalized density profiles for open block cement paste specimens. Bottom of cement paste specimen is at position 28.5 mm (in system coordinates) and top exposed surface is at position 33 mm to 34 mm.

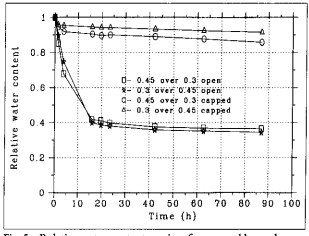

Fig. 5 – Relative water content vs. time for exposed layered cement paste specimens.

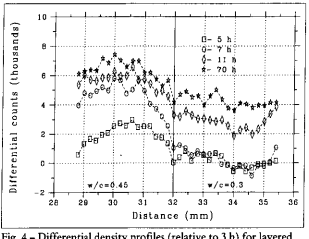

Fig. 4 – Differential density profiles (relative to 3 h) for layered cement paste (0.3 over 0.45) open to the chamber environment. Exposed top surface is at position 35.5 mm.

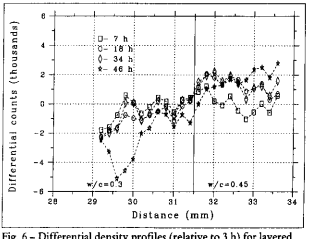

Fig. 6 – Differential density profiles (relative to 3 h) for layered cement paste (0.45 over 0.3) sealed with a cap.

contrast to the inward progression of a relatively sharp drying front often observed in porous materials. While these cement paste specimens are only 4 mm to 5 mm thick, similar results have recently been obtained for cement-based systems 50 mm thick using magnetic resonance imaging [14]. For hardened concrete, Selih *et al.* [15] have observed relatively uniform drying for a few days, followed by the development of a significant moisture gradient originating at the drying surface. In the fresh cement paste, the combination of a relatively wide pore size distribution and a high permeability allows a rapid rearrangement of internal water due to capillary forces, so that the largest pores throughout the specimen thickness empty first. This results in a fairly uniform drying throughout the specimen thickness. The scale over which this mechanism operates in fresh concrete is yet to be determined, but the results of Coussot [14] suggest that it is at least 50 mm, similar to the depth of the steel reinforcement in exposed concrete members. In Fig. 3, it can also be noted that while there is a 1 mm diameter pinhole (collimator) in front of the X-ray detector, the spatial resolution of the system in practice is significantly higher than this as the sharp interfaces present at the tops and bottoms of the specimens seem to be resolvable to the 0.2 mm spacing used in sampling.

Even more interesting are the results for layered composite specimens. For example, Fig.4 shows the differential density profiles for a layered composite consisting of a layer of w/c = 0.3 cement paste over a layer of w/c = 0.45 cement paste. Even though it is the 0.3 cement paste that is exposed to the drying environment, the 0.45 paste "dries out" first (between 3 h and 7 h). Only at later times, after the 0.45 paste has nearly reached complete drying, does the 0.3 paste experience significant water loss. The capillary forces present in the fresh cement paste are easily able to redistribute the water from the lower 0.45 paste layer to the 0.3 paste layer resting on top of it. The results in Fig. 4 are consistent with the mass loss measurements shown in Fig. 5, with a large amount of water loss occurring during the first 10 h to 20 h of exposure, and very little thereafter.

This rearrangement of capillary water is even

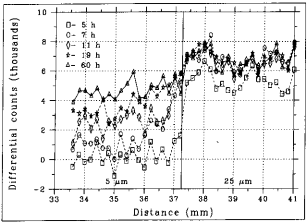

Fig. 7 – Differential density profiles (relative to 3 h) for layered w/c = 0.45 cement paste (25 μm over 5 μm) open to the chamber environment. In this case, the 25 μm cement paste is directly exposed to the environment, with its top surface at position 41 mm.

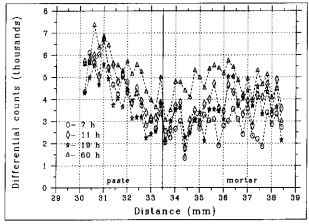

Fig. 9 – Differential density profiles (relative to 3 h) for layered w/c = 0.45 mortar over cement paste open to the chamber environment. In this case, the mortar is directly exposed to the environment, with its top surface at position 38.5 mm.

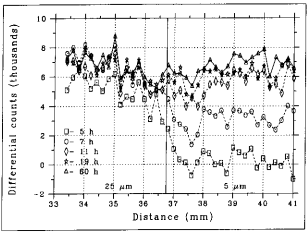

Fig. 8 – Differential density profiles (relative to 3 h) for layered w/c = 0.45 cement paste (5 μm over 25 μm) open to the chamber environment. In this case, the 5 μm cement paste is directly exposed to the environment, with its top surface at position 41 mm.

observed in a capped specimen which loses very little capillary water (only about 10 % over the course of 80 h — see Fig. 5), as shown in Fig. 6. Here, the more dense paste at the bottom of the specimen is seen to further increase in density (negative values on the differential density plot) at the expense of the less dense paste in the top half of the specimen. In this case, a substantial movement of water is observed to occur between 34 h and 46 h as the finer pore structure of the w/c = 0.3 paste imbibes water from the w/c = 0.45 paste to replace that "lost" due to chemical shrinkage/hydration.

Differences in the initial pore size distribution of the fresh cement paste can also be produced at a constant w/c by using cements ground to different finenesses (PSDs). In general, coarser cement particles imply coarser "pores" between them [11]. Figs. 7 and 8 show the results obtained for both configurations of w/c = 0.45 layered composites of the "5 μm" and "25 μm" cements. Regardless of which paste is exposed to the chamber environment, the 25 μm cement paste is always seen to dry out first (3 h to 7 h), while the differential counts for the 5 μm cement paste remain near zero (indicating no loss of water). Once again, the capillary forces draw the water from the coarser pores to the finer ones. Within each layer, however, the drying is still observed to occur uniformly, with no indication of a sharp drying front. Similar experimental observations using magnetic resonance imaging have been made by Coussot *et al.* [16] for composites consisting of layers of packed glass beads of different sizes, once again with equivalent porosities in each layer.

Composite specimens consisting of a layer of cement paste over a layer of mortar and vice versa (at a constant w/c) were also investigated. In these cases, the drying was relatively uniform throughout both layers simultaneously with no clear indication of differential water movement between the layers, as shown in Fig. 9 for a w/c = 0.45 composite. In this case, the coarser pores that most likely exist in the interfacial transition zones (ITZs) surrounding the sand particles in the mortar are balanced by the finer pore structure of the bulk cement paste in the mortar [17]. If the w/c is increased in the ITZs in the mortar, it must also be decreased in the bulk paste relative to the nominal w/c [17]. Thus, most likely, water moves locally from the ITZ to the bulk paste regions within the mortar (which would not be detectable using the X-ray absorption measurements), with little detectable bulk movement from the cement paste to the mortar or vice versa. It should be noted, however, that the observed X-ray absorption results would also be consistent with the mortar being a simple two-phase (paste and sand) composite with no distinguishable ITZ regions. In this case, the cement paste would be nominally identical in the paste and mortar specimens and no differential water movement due to capillary forces would be expected.

Several of the systems studied experimentally were also simulated using the new version of the CEMHYD3D model. For these simulations, the drying rates were chosen to approximately match those observed experimentally (Fig. 5). After each time of hydration, the results were spa-

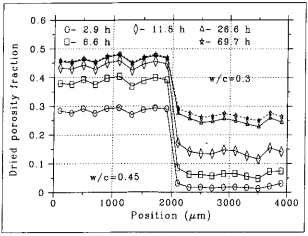

Fig. 10 – Simulation results for "dried" porosity fraction vs. depth for layered composite specimen. Positions 0 to 2000 correspond to the w/c = 0.45 cement paste layer while positions 2000 to 4000 are the w/c = 0.3 paste layer that is directly exposed to the drying environment.

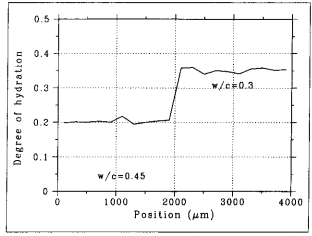

Fig. 12 – Simulation results for degree of hydration vs. depth for layered composite specimen after 70 h of curing. Positions 0 to 2000 correspond to the w/c = 0.45 cement paste layer while positions 2000 to 4000 are the w/c = 0.3 paste layer that is directly exposed to the drying environment.

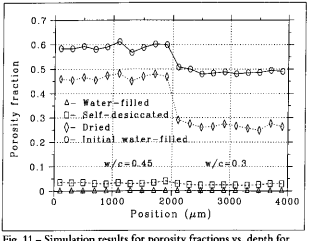

Fig. 11 – Simulation results for porosity fractions vs. depth for layered composite specimen after 70 h of curing. Positions 0 to 2000 correspond to the w/c = 0.45 cement paste layer while positions 2000 to 4000 are the w/c = 0.3 paste layer that is directly exposed to the drying environment. "Initial water-filled" indicates the initial distribution of capillary porosity in the fresh (0 h) cement paste. "Water-filled" indicates the remaining water-filled porosity (after 70 h of curing). "Dried" indicates empty porosity created due to drying, while "Self-desiccated" indicates empty porosity created due to self-desiccation and chemical shrinkage during hydration.

tially averaged over each consecutive 200-pixel thick layer to obtain data with a spatial resolution the same as that of the experimental data, namely 0.2 mm. Figs. 10 and 11 show simulation results for porosity within a 4 mm thick composite specimen consisting of a 2 mm thick layer of w/c = 0.45 cement paste covered by a 2 mm thick layer of w/c = 0.3 cement paste. The similarity between the results in Fig. 10 and their experimental counterpart shown in Fig. 4 can be clearly observed. Because the fresh cement paste has a high permeability and the capillary forces are relatively large (leading to a rapid rearrangement of the water), we can successfully model the drying process by simply emptying the largest pores in the microstructure first without direct consideration of the kinetics of the water movement.

For the simulated system, little drying is observed to occur within the w/c = 0.3 cement paste layer for the first 7 h of exposure, as instead, water is drawn from the w/c = 0.45 cement paste layer underneath it. After 70 h, as shown in Fig. 11, while much more water has dried out from the w/c = 0.45 paste layer, the empty porosity due to self-desiccation is much less and quite similar within the two layers. With the CEMHYD3D model, information on the degree of hydration of the cement paste is also readily available. Fig. 12 shows the degree of hydration obtained after 72 h of hydration as a function of depth. Because it retains water-filled porosity for a longer time period, the w/c = 0.3 cement paste layer is observed to achieve a substantially higher degree of hydration than the w/c = 0.45 cement paste. Results for earlier hydration times such as 3 h (not shown) indicate a much more uniform degree of hydration with depth, as the initial drying and emptying of the largest pores has minimal effects on the initial hydration rate [12, 13].

The computer simulations were also applied to simulating the drying/hydration behavior of the systems with different PSDs. Results for drying profiles are provided in Figs. 13 and 14, while those for simulated degree of hydration are given in Fig. 15. The simulated drying profiles closely mimic their experimental counterpart shown in Fig. 8. Once again, water is seen to be removed preferentially during drying from the coarser pore size distribution microstructure. In this case, the differences in degree of hydration between the two layers (Fig. 15) are even more striking as the 5 μm cement achieves a much higher degree of hydration than the 25 μm cement, due to both its ability to retain water and to its inherently higher hydration rate (because of its smaller size cement particles and higher contents of C_3S and C_3A).

While the model and experimental results compare

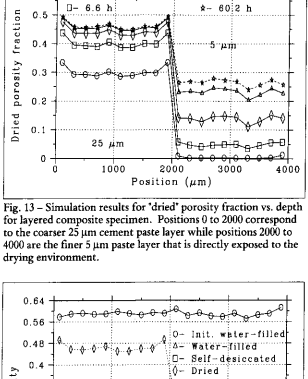

Fig. 13 – Simulation results for "dried" porosity fraction vs. depth for layered composite specimen. Positions 0 to 2000 correspond to the coarser 25 μm cement paste layer while positions 2000 to 4000 are the finer 5 μm paste layer that is directly exposed to the drying environment.

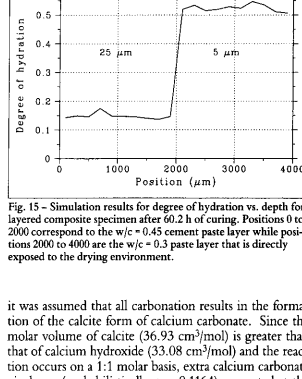

Fig. 15 – Simulation results for degree of hydration vs. depth for layered composite specimen after 60.2 h of curing. Positions 0 to 2000 correspond to the w/c = 0.45 cement paste layer while positions 2000 to 4000 are the w/c = 0.3 paste layer that is directly exposed to the drying environment.

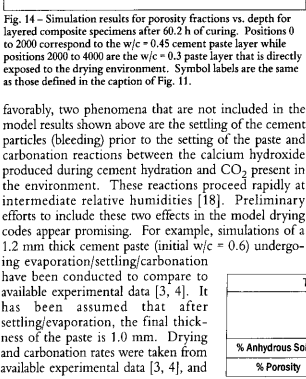

Fig. 14 – Simulation results for porosity fractions vs. depth for layered composite specimens after 60.2 h of curing. Positions 0 to 2000 correspond to the w/c = 0.45 cement paste layer while positions 2000 to 4000 are the w/c = 0.3 paste layer that is directly exposed to the drying environment. Symbol labels are the same as those defined in the caption of Fig. 11.

favorably, two phenomena that are not included in the model results shown above are the settling of the cement particles (bleeding) prior to the setting of the paste and carbonation reactions between the calcium hydroxide produced during cement hydration and CO_2 present in the environment. These reactions proceed rapidly at intermediate relative humidities [18]. Preliminary efforts to include these two effects in the model drying codes appear promising. For example, simulations of a 1.2 mm thick cement paste (initial w/c = 0.6) undergoing evaporation/settling/carbonation have been conducted to compare to available experimental data [3, 4]. It has been assumed that after settling/evaporation, the final thickness of the paste is 1.0 mm. Drying and carbonation rates were taken from available experimental data [3, 4], and it was assumed that all carbonation results in the formation of the calcite form of calcium carbonate. Since the molar volume of calcite (36.93 cm^3/mol) is greater than that of calcium hydroxide (33.08 cm^3/mol) and the reaction occurs on a 1:1 molar basis, extra calcium carbonate pixels are (probabilistically, p = 0.1164) generated at the reaction sites to maintain the appropriate volume stoichiometry for the carbonation reaction. Also, the water released from the calcium hydroxide during carbonation is made available for further hydration of the cement.

A comparison of the experimental scanning electron microscopy/image analysis (SEM/IA) results for capillary porosity and the ratio of anhydrous cement to solid material (anhydrous cement + hydration products) [4] to those based on the simulations of varying complexity are provided in Table 1. It is observed that the best quantitative agreement is observed when both settling and carbonation are included in the model hydration/drying codes. Thus, the development and evaluation of these enhanced codes will be the subject of future research.

Finally, Figs. 16 and 17 provide three-dimensional microstructures from the top surface and an interior 100 pixel x 100 pixel x 100 pixel section of a simulated 1 mm thick w/c = 0.6 microstructure (no settling or carbonation). In these figures, empty porosity is white, water-filled porosity is dark grey, and the unhydrated cement particles are light grey. In comparing the two images, one can definitely observe the preferential drying at the immediate top surface (due to the larger pores present there) and a more "uniform" drying within the

Table 1 – Hydration models of varying complexity

	Experimental (SEM/IA)	Hydration + Evaporation	Hydration + Evaporation + Settling	Hydration + Evaporation + Settling/Carbonation
% Anhydrous Solids	40.	38.	48.	43.
% Porosity	40.	50.	44.	46.

ACKNOWLEDGEMENTS

Some of the measurements presented here were performed during the summer of 1999, when D. P. Bentz was a visiting professor at the Department of Structural Engineering and Materials, DTU, funded by the Knud Hojgaard Foundation. The authors would like to thank Dr. Claus-Jochen Haecker of Dyckerhoff Zement for supplying the cements ground to the two extremes of fineness. D. P. Bentz would also like to acknowledge fruitful discussions with Dr. Daniel Quenard of Centre Scientifique et Technique du Bâtiment, Grenoble, France and to thank his wife, Janet Carey-Bentz, for the idea of using the Lego blocks as sample holders. Partial funding for this research was provided by the NIST Partnership for High Performance Concrete Technology (PHPCT) program.

REFERENCES

[1] Meeks, K. W. and Carino, N. J., 'Curing of High-Performance Concrete: Report of the State-of-the-art', NISTIR 6295, U.S. Department of Commerce, March 1999.

[2] Griesel, E. J., 'The influence of controlled environmental conditions on the potential durability of concrete', M.S. Thesis, University of Stellenbosch, South Africa, April 1999.

[3] Vallée, F., Lejeune, C. and Cope, R., 'Investigation of the evolution of a thin layer cement paste microstructure during climatic exposures', submitted to *Cem. Concr. Res.*, 2000.

[4] Vallée, F., 'Durabilité des composites polymères/ciment: Application au cas des enduits minces sur isolants', Ph.D. thesis, Institut National Polytechnique de Grenoble, France, October 1999.

[5] Hansen, K. K., Jensen, S. K., Gerward, L. and Singh, K., 'Dual-energy X-ray absorptiometry for the simultaneous determination of density and moisture content in porous structural materials', in 'Proc. of the 5th Symposium on Building Physics in the Nordic Countries', (Chalmers University of Technology, Gothenburg, Sweden, 1999) 281-288.

[6] Bentz, D. P., 'Three-dimensional computer simulation of cement hydration and microstructure development', *J. Amer. Ceram. Soc.* **80** (1) (1997) 3-21.

[7] Bentz, D. P., 'CEMHYD3D: A three-dimensional cement hydration and microstructure development modelling package. Version 2.0', NISTIR 6485, U.S. Department of Commerce, April 2000, available at http://ciks.cbt.nist.gov/monograph.

[8] Bentz, D. P. and Hansen, K. K., 'Preliminary observations of water movement in cement pastes during curing using X-ray absorption', *Cem. Concr. Res.* **30** (2000) 1157-1168.

[9] Madsen, H. M., 'Hydration and drying in cement pastes measured with X-ray', M.S. Thesis, Technical University of Denmark, Lyngby, Denmark, February 2000 (in Danish).

[10] Cement and Concrete Reference Laboratory Proficiency Sample Program: Final Report Portland Cement Proficiency Samples Number 133 and Number 134, Cement and Concrete Reference Laboratory, September, 1999.

[11] Bentz, D. P., Jensen, O. M., Hansen, K. K., Olesen, J. F., Stang, H. and Haecker, C. J., 'Influence of cement particle size distribution on early age autogenous strains and stresses in cement-based materials', *J. Amer. Ceram. Soc.* **84** (1) (2001) 129-135.

[12] Bentz, D. P., Snyder, K. A. and Stutzman, P. E., 'Microstructural modelling of self-desiccation during hydration', in 'Self-Desiccation and Its Importance in Concrete Technology', Ed. B. Persson and G. Fagerlund (Lund Institute of Technology, Lund, Sweden, 1997) 132-140.

[13] Bentz, D. P., 'Effects of cement PSD on porosity percolation and self-desiccation', in 'Self-Desiccation and Its Importance in Concrete Technology II', Ed. B. Persson and G. Fagerlund (Lund Institute of Technology, Lund, Sweden, 1999) 127-135.

[14] Coussot, P., private communication, 1999.

[15] Selih, J., Sousa, A. C. M. and Bremner, T. W., 'Moisture transport in initially saturated concrete during drying', *Transport in Porous Media* **24** (1996) 81-106.

[16] Coussot, P., Gauthier, C., Nadji, D., Borgotti, J.-C., Vie, P. and Bertrand, F., 'Mouvements capillaires durant le séchage d'une pâte granulaire', C.R. Acad. Sci. (Paris), t. 327, Serie IIb (1999) 1101-1106.

[17] Bentz, D. P. and Garboczi, E. J., 'Computer modelling of interfacial transition zone microstructures and properties', in 'Engineering and Transport Properties of the Interfacial Transition Zone in Cementitious Composites', Ed. M. G. Alexander, G. Arliguie, G. Ballivy, A. Bentur and J. Marchand (RILEM, Paris, France, 1999) 349-385.

[18] Taylor, H. F. W., 'Cement Chemistry' (Thomas Telford, London 1997).

[19] Weber, S. and Reinhardt, H. W., 'Manipulating the water content and microstructure of high performance concrete using autogenous curing', in 'Modern Concrete Materials: Binders, Additions, and Admixtures', Ed. R. K. Dhir and T. D. Dyer (Thomas Telford, London, 1999) 567-577.

[20] Bentz, D. P. and Snyder, K. A., 'Protected paste volume in concrete: extension to internal curing using saturated lightweight fine aggregate', *Cem. Concr. Res.* **29** (11) (1999) 1863-1867.